

Jussi Salmi, Andreas Richter, and Visa Koivunen. 2006. State-space modeling and propagation parameter tracking: Multitarget tracking based approach. In: Michael B. Matthews (editor). Conference Record of the 40th Asilomar Conference on Signals, Systems and Computers (ACSSC 2006). Pacific Grove, CA, USA. 29 October - 1 November 2006, pages 941-945.

© 2006 IEEE

Reprinted with permission.

This material is posted here with permission of the IEEE. Such permission of the IEEE does not in any way imply IEEE endorsement of any of Helsinki University of Technology's products or services. Internal or personal use of this material is permitted. However, permission to reprint/republish this material for advertising or promotional purposes or for creating new collective works for resale or redistribution must be obtained from the IEEE by writing to [pubs-permissions@ieee.org](mailto:pubs-permissions@ieee.org).

By choosing to view this document, you agree to all provisions of the copyright laws protecting it.

# State-Space Modeling and Propagation Parameter Tracking: Multitarget tracking based approach

Jussi Salmi, Andreas Richter and Visa Koivunen  
 Signal Processing Laboratory/SMARAD CoE  
 Helsinki University of Technology  
 Espoo, Finland

**Abstract**—The paper describes a state-space approach for retrieving the parameters of the double directional MIMO propagation channel model from channel sounding measurements. We address the issues arising from tracking a varying number of jointly estimated targets (propagation paths) from a vast amount of data. We focus on state dimensionality estimation, i.e., how to drop paths from the state as well as augmenting the state with new path estimates. We propose a whiteness test for detecting the time instances when to increase the number of paths to track. Simulation results are presented to illustrate the benefits of the path detection algorithm.

## I. INTRODUCTION

In this paper we discuss a parameter estimation application, namely the estimation of the parameters of concentrated propagation paths of the double-directional radio channel model from MIMO (Multiple-Input-Multiple-Output) measurements. The measurements and their analysis plays a crucial role in the development of increasingly accurate modeling of radio wave propagation. The modeling is needed for the development of future communication systems [1] utilizing the spatial degrees of freedom offered by the radio propagation environment.

The extraction of the channel model parameters from the measurement data is done using a parameter estimation algorithm, such as SAGE [2] or RIMAX [3]. A straight-forward approach for estimating the radio channel parameters (such as propagation path delays, angles of arrival and departure, polarized path weight components) is to estimate them for each snapshot independently. However, it can be observed from measurements, that the specular component of the radio channel contains typically propagation paths, which persist over a relatively large number of snapshots (time). Also, the parameters of these paths vary slowly in time (with respect to the measurement interval). This observation can be exploited to track the path parameters over time in order to reveal dynamic properties of the radio channel. Furthermore, sequential computation usually reduces complexity of the estimator.

In this paper we use a state-space approach for tracking the radio propagation path parameters in time. This is done by using a state-space model based on the nonlinear data model presented in [3], and applying an Extended Kalman Filter (EKF) for parameter estimation. The approach for propagation path parameter estimation using Kalman filtering was

The research was partly funded by the WILATI project. First author would like to thank the Finnish Technology Promotion Foundation (TES) and Emil Aaltonen Foundation for financial support.

introduced in [4]. The method was extended and applied to real world measurements in [5]. In [6] the state-space model of [5] was enhanced, and also the model order selection problem was addressed. In this paper we refine the model order selection by introducing a CUSUM based whiteness test to improve the detection of new paths.

The paper is organized as follows. Section II describes the channel sounding procedure briefly, and provides the necessary expressions to express the measurements using state-space modeling. In Section III we describe the estimation procedure including the EKF and the state dimension determination. Section IV presents the simulation results, and Section V concludes the paper.

## II. SYSTEM AND MODEL DESCRIPTION

A radio channel sounder measures the complex channel response (either in time or frequency domain) sequentially for each  $M_t$  transmit (Tx) and  $M_r$  receive (Rx) antenna pairs at a time. The measurement can take place either in time- or frequency domain. The channel sounder at Helsinki University of Technology (TKK) uses a pseudo noise (PN) code generator at Tx. The number of channels is  $M_t \cdot M_r = 32 \cdot 32$ , and the length of the measured impulse responses is  $M_f = 510$ . This results in  $M = M_f M_t M_r \approx 5 \cdot 10^5$  complex samples per measurement cycle (observation). A single observation takes  $\sim 8.7$  ms to measure. Another example is the Medav's RUSK sounder, which relies on the multi carrier spread spectrum technique. More about channel sounding can be found in [7]. One should note that all state of the art channel sounders use the same basic principle of fast correlation based network analyzers. Therefore the models described in the following are applicable to both of the aforementioned sounder architectures.

### A. Double Directional MIMO Channel Model

To extract the spatial and temporal information of the MIMO radio channel from the measurements we use the double directional channel model [8]. The frequency response of the channel with the antenna arrays is expressed as a superposition of  $P$  propagation paths

$$H(f) = \sum_{p=1}^P \{ \mathbf{B}_R(\varphi_{R,p}, \vartheta_{R,p}) \cdot \begin{bmatrix} \gamma_{HH,p} & \gamma_{HV,p} \\ \gamma_{VH,p} & \gamma_{VV,p} \end{bmatrix} \cdot \mathbf{B}_T(\varphi_{T,p}, \vartheta_{T,p})^T \cdot e^{-j2\pi f \tau_p} \}, \quad (1)$$

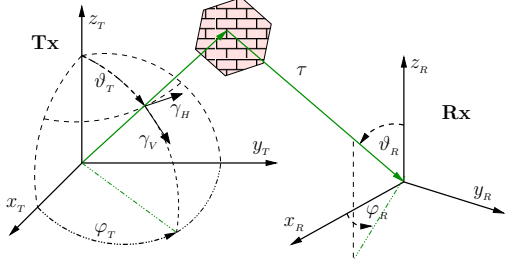


Fig. 1. The double directional radio channel model parameters for a single propagation path. Tx denotes transmitter and Rx receiver.

where  $\mathbf{B}_R$  and  $\mathbf{B}_T$  are the nonlinear mappings of the angles of arrival ( $\varphi_R, \vartheta_R$ ) and departure ( $\varphi_T, \vartheta_T$ ) to the antenna array responses. The parameter  $\tau$  denotes the time delay of arrival of a path, and  $\gamma_i$  are the radio wave polarization coefficients (Horizontal-to-Horizontal, Horizontal-to-Vertical, etc.). The meaning of the propagation path parameters is illustrated in Fig. 1.

### B. State-Space Model

State-space modeling of the radio channel propagation parameters is based on the assumption that the parameters evolve slowly (w.r.t. the measurement interval) over time and are correlated in subsequent time instances. Then the process can be described using a Gauss-Markov model, i.e., the probability (density) of the next state  $\theta_{k+1}$  depends only on the current state  $p(\theta_{k+1}|\theta_k, \theta_{k-1} \dots \theta_0) = p(\theta_{k+1}|\theta_k)$ , and is Gaussian distributed.

The state-space model used in this paper consist of the state equation, describing the dynamic behavior of the propagation parameters of  $P_k$  paths, and the nonlinear measurement equation, mapping the double-directional model (1) parameters to the channel sounder output data.

### C. State Equations

The state in our model is comprised of the structural parameters

$$\boldsymbol{\mu} = [\boldsymbol{\tau}^T \boldsymbol{\varphi}_T^T \boldsymbol{\vartheta}_T^T \boldsymbol{\varphi}_R^T \boldsymbol{\vartheta}_R^T]^T \in \mathbb{R}^{5P \times 1}, \quad (2)$$

related to the propagation environment geometry, the rate of change of the structural parameters  $\Delta\boldsymbol{\mu}$ , and the path weight parameters

$$\boldsymbol{\gamma} = [\boldsymbol{\gamma}_{HH}^T \boldsymbol{\gamma}_{HV}^T \boldsymbol{\gamma}_{VH}^T \boldsymbol{\gamma}_{VV}^T]^T \in \mathbb{C}^{4P \times 1}. \quad (3)$$

The path weight parameters are the magnitude  $\alpha_i = \log_e(|\gamma_i|)$  in logarithmic scale, and the phase  $\omega_i = \arg(\gamma_i)$ , i.e.,  $\gamma_i = e^{\alpha_i + j\omega_i}$ . Another option is to use the real and imaginary parts of the path weights, but tracking of these becomes impossible at our measurement rate.

The state vector at time  $k$  is given by

$$\boldsymbol{\theta}_k = [\boldsymbol{\tau}^T \Delta\boldsymbol{\tau}^T \boldsymbol{\varphi}_T^T \Delta\boldsymbol{\varphi}_T^T \boldsymbol{\vartheta}_T^T \Delta\boldsymbol{\vartheta}_T^T \boldsymbol{\varphi}_R^T \Delta\boldsymbol{\varphi}_R^T \boldsymbol{\vartheta}_R^T \Delta\boldsymbol{\vartheta}_R^T \boldsymbol{\alpha}_{HH}^T \boldsymbol{\omega}_{HH}^T \boldsymbol{\alpha}_{HV}^T \boldsymbol{\omega}_{HV}^T \boldsymbol{\alpha}_{VH}^T \boldsymbol{\omega}_{VH}^T \boldsymbol{\alpha}_{VV}^T \boldsymbol{\omega}_{VV}^T]^T,$$

i.e., the number of parameters per path in the state is  $L = 18$ . In our application the observation interval is constant. The choice of parameters enables us to utilize the time dependency of the structural propagation path parameters in the state transition equation

$$\boldsymbol{\theta}_k = \boldsymbol{\Phi}\boldsymbol{\theta}_{k-1} + \mathbf{v}_k,$$

where  $\mathbf{v}_k \sim \mathcal{N}(\mathbf{0}, \mathbf{Q})$  is the state noise with (diagonal) covariance matrix  $\mathbf{Q}$ . The state transition matrix  $\boldsymbol{\Phi}$  is chosen to provide linear prediction  $\boldsymbol{\mu}_{k|k-1} = \boldsymbol{\mu}_{k|k-1} + \Delta\boldsymbol{\mu}_{k-1|k-1}$  of the structural parameters.

### D. Measurement Equations

The structural parameters (2) are related to the channel sounder output through a complex shift operation [3]

$$\mathbf{A}(\boldsymbol{\mu}_i) = \begin{bmatrix} e^{-j(-\frac{N_i-1}{2})\mu_{i,1}} \dots e^{-j(-\frac{N_i-1}{2})\mu_{i,P}} \\ \vdots \\ e^{-j(+\frac{N_i-1}{2})\mu_{i,1}} \dots e^{-j(+\frac{N_i-1}{2})\mu_{i,P}} \end{bmatrix} \in \mathbb{C}^{N_i \times P}. \quad (4)$$

The shift matrices  $\mathbf{A}_i$  are multiplied by the corresponding system responses  $\mathbf{G}_i \in \mathbb{C}^{M_i \times N_i}$  (provided by calibration measurements), yielding<sup>1</sup>

$$\begin{aligned} \mathbf{B}_f &= \mathbf{G}_f \cdot \mathbf{A}(\boldsymbol{\tau}) && \in \mathbb{C}^{M_f \times P} \\ \mathbf{B}_{RH} &= \mathbf{G}_{RH} \cdot (\mathbf{A}(\boldsymbol{\vartheta}_R) \diamond \mathbf{A}(\boldsymbol{\varphi}_R)) && \in \mathbb{C}^{M_R \times P} \\ \mathbf{B}_{RV} &= \mathbf{G}_{RV} \cdot (\mathbf{A}(\boldsymbol{\vartheta}_R) \diamond \mathbf{A}(\boldsymbol{\varphi}_R)) && \in \mathbb{C}^{M_R \times P} \\ \mathbf{B}_{TH} &= \mathbf{G}_{TH} \cdot (\mathbf{A}(\boldsymbol{\vartheta}_T) \diamond \mathbf{A}(\boldsymbol{\varphi}_T)) && \in \mathbb{C}^{M_T \times P} \\ \mathbf{B}_{TV} &= \mathbf{G}_{TV} \cdot (\mathbf{A}(\boldsymbol{\vartheta}_T) \diamond \mathbf{A}(\boldsymbol{\varphi}_T)) && \in \mathbb{C}^{M_T \times P}. \end{aligned} \quad (5)$$

The system functions  $\mathbf{G}_{(R/T)(H/V)}$  for the antenna array responses are calculated from antenna calibration measurements using the Effective Aperture Distribution Function (EADF) [7]. This allows numerically effective and differentiable representation of the antenna beam patterns through a 2D-Fourier series expansion. To obtain the frequency response  $\mathbf{G}_f$  of the system a back-to-back cable calibration measurement is required.

Given the expressions for the basis functions (5) we introduce the matrix valued function  $\mathbf{B}(\boldsymbol{\mu}) \in \mathbb{C}^{M \times 4P}$

$$\mathbf{B}(\boldsymbol{\mu}) = \begin{bmatrix} \mathbf{B}_{RH} \diamond \mathbf{B}_{TH} \diamond \mathbf{B}_f & \mathbf{B}_{RV} \diamond \mathbf{B}_{TH} \diamond \mathbf{B}_f \dots \\ \mathbf{B}_{RH} \diamond \mathbf{B}_{TV} \diamond \mathbf{B}_f & \mathbf{B}_{RV} \diamond \mathbf{B}_{TV} \diamond \mathbf{B}_f \end{bmatrix}. \quad (6)$$

Using (3) and (6) the propagation path parameters  $\boldsymbol{\mu}$  and  $\boldsymbol{\gamma}$  are mapped to an observation vector of length  $M = M_f M_T M_R$  with the double-directional channel model (sampled version of (1)) as

$$\mathbf{s}(\boldsymbol{\mu}, \boldsymbol{\gamma}) = \mathbf{B}(\boldsymbol{\mu}) \cdot \boldsymbol{\gamma} \in \mathbb{C}^{M \times 1}. \quad (7)$$

The nonlinear measurement equation is given by

$$\mathbf{y}_k = \mathbf{s}(\boldsymbol{\theta}_k) + \mathbf{n}_{y,k} \in \mathbb{C}^{M \times 1},$$

where  $\mathbf{s}(\boldsymbol{\theta}_k)$  is the mapping of the propagation paths parameters to the observation (7), and  $\mathbf{n}_{y,k} \sim \mathcal{N}(\mathbf{0}, \mathbf{R}_{dmc})$

<sup>1</sup>  $\diamond$  denotes the Khatri-Rao product (column-wise Kronecker-product).

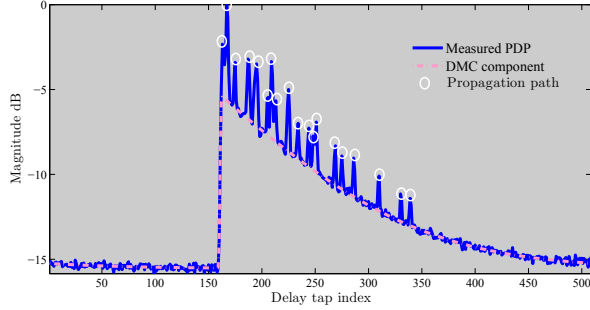


Fig. 2. Illustration of a power delay profile using the division to the concentrated propagation paths and the dense multipath component.

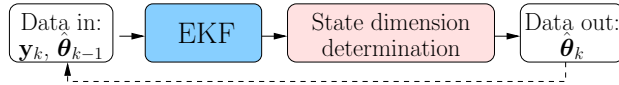


Fig. 3. Estimation procedure principle. The state vector  $\hat{\theta}_{k-1}$  (as well as other EKF system matrices) of previous time instant may have different dimensions than the current one  $\hat{\theta}_k$ .

is a colored noise process with a known covariance matrix  $\mathbf{R}_{dmc}$ . This noise process consists not only of white Gaussian measurement noise, but also of the dense multipath component (DMC) [3]. The DMC is caused by the distributed diffuse scattering in the radio channel resulting in an exponentially decaying (with delay) Power Delay Profile (PDP). Fig. 2 illustrates a realization of a PDP (squared complex impulse response) averaged over  $M_t M_r$  channels.

The DMC component is assumed to be a white process in the angular domain and independent at both link ends. This assumption leads to the covariance structure

$$\mathbf{R}_{dmc} = \mathbf{R}_T \otimes \mathbf{R}_R \otimes \mathbf{R}'_f + \alpha_0 \mathbf{I} = \mathbf{I}_T \otimes \mathbf{I}_R \otimes \mathbf{R}_f, \quad (8)$$

where  $\alpha_0$  denotes the measurement noise variance and  $\mathbf{R}_f = \mathbf{R}'_f + \alpha_0 \mathbf{I}$ . This structure makes the implementation of the EKF feasible, because the inversion of  $\mathbf{R}_{dmc}^{-1}$  requires now only inverting the  $M_f \times M_f$  matrix  $\mathbf{R}_f$ . In this paper we assume  $\mathbf{R}_f$  known. The estimation and tracking of the DMC parameters (using the EKF) is discussed in [9] and [10], where the latter extends the model to a nonwhite distribution also in angular domain ( $\mathbf{R}_T$  and  $\mathbf{R}_R$ ).

### III. PROPAGATION PATH PARAMETER ESTIMATION

The proposed parameter estimation procedure consists of the following components. The core of the algorithm, tracking the propagation path parameters over time, is the EKF. After the EKF the reliability of the estimated paths is evaluated. The path estimates that fail the designated criterion are then dropped from the state. To check if the model order  $P_k$  is high enough, we propose a CUSUM [11] based whiteness test in the delay domain. The general principle of the estimation procedure is presented in Fig. 3.

#### A. Extended Kalman Filter

The propagation parameters are tracked using the Extended Kalman Filter. The EKF uses Taylor series expansion to

linearize the nonlinear data model about the current estimates. To apply the EKF one needs to compute the first order partial derivatives to the parameters  $\theta$  of the data model  $s(\theta)$ , i.e., the Jacobian matrix  $\mathbf{D}(\theta) = \partial/\partial\theta^T (s(\theta))$ , which is derived in [3]. We use the ‘‘Alternative form of the discrete Kalman filter’’ [12], allowing some algebraic simplifications. The equations can be summarized as

$$\hat{\theta}_{(k|k-1)} = \Phi \hat{\theta}_{(k-1|k-1)} \quad (9)$$

$$\mathbf{P}_{(k|k-1)} = \Phi \mathbf{P}_{(k-1|k-1)} \Phi^T + \mathbf{Q}_k \quad (10)$$

$$\mathbf{P}_{(k|k)} = \left( \mathbf{P}_{(k|k-1)}^{-1} + \mathbf{D}_k^H \mathbf{R}_k^{-1} \mathbf{D}_k \right)^{-1} \quad (11)$$

$$\mathbf{K}_k = \mathbf{P}_{(k|k)} \mathbf{D}_k^H \mathbf{R}_k^{-1} \quad (12)$$

$$\hat{\theta}_{(k|k)} = \hat{\theta}_{(k|k-1)} + \mathbf{K}_k \left( \mathbf{y}_k - s \left( \hat{\theta}_{(k|k-1)} \right) \right), \quad (13)$$

where the Jacobian is evaluated as  $\mathbf{D}_k = \mathbf{D}(\hat{\theta}_{(k|k-1)})$ . Equations (11-13) can be expressed in terms of the score function of maximum likelihood estimation [3]

$$\begin{aligned} \mathbf{q}(\mathbf{y}|\theta, \mathbf{R}) &= \frac{\partial}{\partial \theta} \mathcal{L}(\mathbf{y}|\theta, \mathbf{R}) \\ &= 2 \cdot \Re \left\{ \mathbf{D}^H(\theta) \mathbf{R}^{-1} (\mathbf{y} - \mathbf{s}(\theta)) \right\}, \end{aligned} \quad (14)$$

and the Fisher information matrix [3]

$$\begin{aligned} \mathbf{J}(\theta, \mathbf{R}) &= -\mathbf{E} \left\{ \frac{\partial}{\partial \theta} \mathcal{L}(\mathbf{y}|\theta, \mathbf{R}) \left( \frac{\partial}{\partial \theta} \mathcal{L}(\mathbf{y}|\theta, \mathbf{R}) \right)^T \right\} \\ &= 2 \cdot \Re \left\{ \mathbf{D}^H(\theta) \mathbf{R}^{-1} \mathbf{D}(\theta) \right\}. \end{aligned} \quad (15)$$

This simplifies (11) and (13) as

$$\begin{aligned} \mathbf{P}_{(k|k)} &= \left( \mathbf{P}_{(k|k-1)}^{-1} + \mathbf{J}(\hat{\theta}_{(k|k-1)}, \mathbf{R}_k) \right)^{-1} \\ \hat{\theta}_{(k|k)} &= \hat{\theta}_{(k|k-1)} + \mathbf{P}_{(k|k)} \mathbf{q} \left( \mathbf{y}_k | \hat{\theta}_{(k|k-1)}, \mathbf{R}_k \right). \end{aligned}$$

The structure of the data model (equations (6) and (8)) allows for several computational simplifications for computing  $\mathbf{J}(\theta, \mathbf{R}_k)$  and  $\mathbf{q}(\mathbf{y}_k|\theta, \mathbf{R}_k)$  as suggested in [3].

#### B. State Dimensionality Determination

Due to the nature of the dynamic radio channel new propagation paths may arise, as well as old paths disappear during the measurements. Therefore adaptation of the state dimensionality is required over time. In this section we describe a two stage procedure for determining the state dimension. This procedure comprises of dropping insignificant paths and detecting new paths.

In the first step the significance of the paths currently being tracked by the EKF is evaluated. This is done the statistical Wald hypothesis test [13] with the estimated variance of the magnitude of the path weights as the test statistics (see [6] for details). The threshold value for the hypothesis that a path is significant can then be selected as a confidence level of a  $\chi^2$  distribution. If a path is considered insignificant, its corresponding elements are removed from the state vector  $\hat{\theta}_{(k|k)}$ , and the filtering error covariance matrix  $\mathbf{P}_{(k|k)}$ .

The second step, i.e. the detection of new path parameters is investigated here more thoroughly. The first approach described in [6] is to simply compute the residual sequence

$$\tilde{\mathbf{y}}_k = \mathbf{y}_k - \mathbf{s}(\boldsymbol{\theta}_{(k|k)}), \quad (16)$$

and feed it to the RIMAX [3] algorithm, which would do a coarse grid search and an iterative ML optimization for a given number of new path estimates  $P_{new}$ . This is problematic in two senses. First of all, it is usually unnecessary as well as computationally tedious to run the search for new paths “blindly” for each observation. Secondly, a fixed number  $P_{new} = P_{new}^0$ , which typically has to be chosen to overestimate the actual requirement, is used for the initial number of new paths to search from the grid<sup>2</sup>.

In the following we propose an approach based on a whiteness based change detection (CUSUM [11]) algorithm to address both of the aforementioned deficiencies. Intuitively this test checks whether its test statistic  $g_k = g_{k-1} + f_k - d$ , is resulting from white noise input  $f_k$ . The drift  $d$  is subtracted to avoid random walk. If  $g_k$  exceeds threshold  $h$ , an alarm is given and the test is reset.

We apply the test to each delay bin as follows. For each observation  $k$  (the subscript  $k$  is dropped from the expressions for convenience), we apply whitening to the residual vector (16), using the Cholesky decomposition of the measurement covariance matrix  $\mathbf{R}_f = \mathbf{L}_f \mathbf{L}_f^H$ . The resulting matrix  $\mathbf{Z}_f \in \mathbb{C}^{M_f \times M_t M_r}$  is given by<sup>3</sup>

$$\mathbf{Z}_f = \mathbf{L}_f^{-1} \cdot \text{mat} \{ \tilde{\mathbf{y}}_k, M_f, M_t M_r \}. \quad (17)$$

Due to the whitening,  $\mathbf{Z}_f$  cannot be transformed to delay domain using a straight-forward IDFT. Instead, let us define a whitened DFT matrix

$$\mathbf{A}_w = \mathbf{L}_f^{-1} \mathbf{A}_{DFT} \in \mathbb{C}^{M_f \times M_f}, \quad (18)$$

where  $\mathbf{A}_{DFT}$  is defined as (4) with  $N = M_f$  points. Normalizing the columns of  $\mathbf{A}_w$  gives

$$\tilde{\mathbf{A}}_w = \mathbf{A}_w (\mathbf{A}_w^H \mathbf{A}_w \odot \mathbf{I})^{-\frac{1}{2}}, \quad (19)$$

which can be then applied to (17), yielding the delay domain expression

$$\mathbf{Z}_\tau = \tilde{\mathbf{A}}_w^H \mathbf{Z}_f. \quad (20)$$

The elements of  $\mathbf{Z}_\tau$  are then squared and summed over the second dimension (i.e., all the  $M_t M_r$  spatial channels). The resulting test vector  $\mathbf{f}_k$  is given by<sup>4</sup>

$$\mathbf{f}_k = \frac{1}{\sqrt{M_t M_r}} \text{diag} \{ \mathbf{Z}_\tau \mathbf{Z}_\tau^H \} - \sqrt{M_t M_r} \in \mathbb{R}^{M_f \times 1}. \quad (21)$$

The normalization yields that each element of  $\mathbf{f}_k$  is drawn from  $\mathcal{N}(0, 1)$  distribution (exact distribution being a  $\chi^2$  with

<sup>2</sup>The number of new estimates is finally determined by the ML optimization.

<sup>3</sup>The operator  $\text{mat} \{ \mathbf{a}, N_1, N_2 \}$  forms a  $N_1 \times N_2$  matrix out of a  $N_1 \cdot N_2$  length vector  $\mathbf{a}$  by taking the first  $N_1$  elements as the first column, second  $N_1$  elements as the second column, etc., up to the  $N_2^{\text{th}}$  set of  $N_1$  elements as the last column.

<sup>4</sup>The operator  $\text{diag} \{ \bullet \}$  returns the diagonal values of  $\bullet$  in a column vector.

$M_t \cdot M_r$  degrees of freedom), under the hypothesis there are no additional paths in the residual (assuming perfect whitening). Given  $\mathbf{f}_k$ , we update the  $i^{\text{th}}$  element of the CUSUM vector  $\mathbf{g}_k \in \mathbb{R}^{M_f \times 1}$  by adding the current  $f_{k,i}$  value and subtracting a drift parameter  $d$  as

$$g_{k,i} = \max \{ (g_{k-1,i} + f_{k,i} - d), 0 \}. \quad (22)$$

In this one sided test the CUSUM values  $g_{k,i}$  are not allowed to go below zero. The drift  $d$  is subtracted from  $g_{k,i}$  to prevent random walk [11].

The search for new paths is based on setting a threshold  $h$  for the elements in  $\mathbf{g}_k$ . At each time instant  $k$  the search for new paths is performed in the vicinity of the delay bins corresponding to the  $\mathbf{g}_k$  values exceeding the threshold  $h$ . The selection of the values for  $d$  and  $h$  is a compromise between the probability of false detection vs. probability of missing a weak path. The drift  $d$  can also compensate for some model mismatch, e.g., if the estimate for  $\mathbf{R}_f$  is poor. More on selecting these values can be found in [11].

#### IV. SIMULATION RESULTS

A simulation was performed to compare two path detection approaches. Approach A1 is one where a fixed number of new paths (in this simulation  $P_{new} = 5$ ) is searched for at each time instant [6], and Approach A2 is the proposed CUSUM path detection described in Section III-B. For A2 we selected  $d = 2$  (corresponding approximately 98% confidence level of  $\mathcal{N}(0, 1)$  distribution) as the drift, and  $h = 4$  as the threshold parameters.

In the simulation we use EADF’s of a real 8-element dual polarized uniform linear array as a receiver (access point) and a real 16-element uniform circular array as a transmitter (user). The simulation is run for 300 snapshots in an environment with 10-30 propagation paths shown by the solid blue line in the lower part of Fig. 6. The path parameters are derived using randomly placed scatterers in an area around the receiver (a single-bounce model). The magnitudes of the path weights fade in/out gradually (seen as darker colors in Fig. 5) as the paths appear/disappear. The phase and magnitude (as well as delay of arrival) of the paths depend on the path length. Fast and slow fading of the path weights are neglected, but measurement noise as well as DMC is included in the simulation. An example of the power delay profile of a simulated observation is shown in Fig. 4.

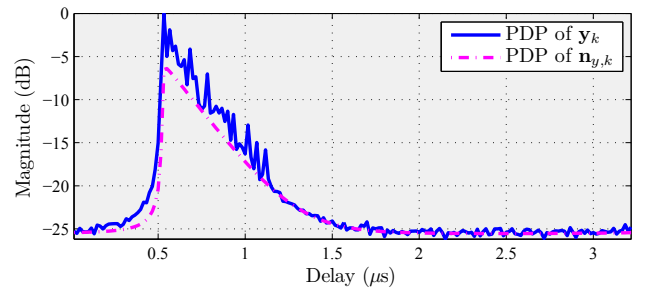


Fig. 4. Example PDP of a simulated observation with 30 paths.

Fig. 5 shows a comparison between the true azimuth angles at the transmitter and the estimates from the two approaches A1 and A2 (only one parameter dimension illustrated due to limited space). It can be observed that both capture the

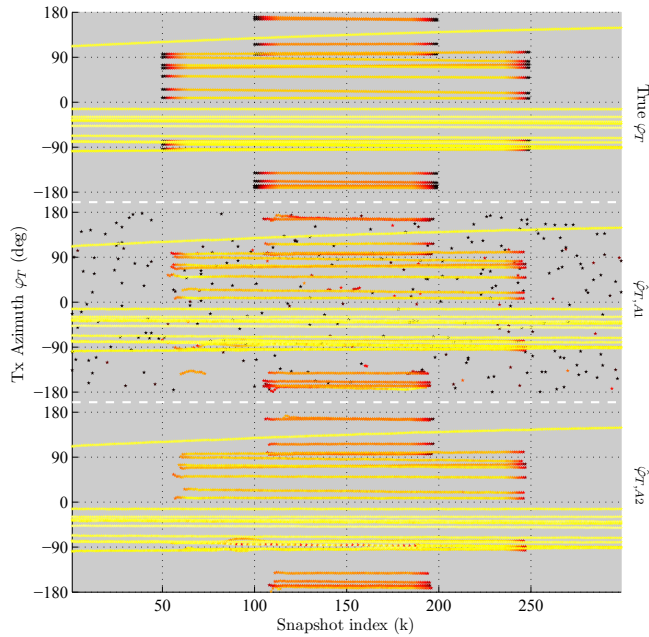


Fig. 5. Azimuth Tx (user) angles in the simulation for 10-30 paths. The lighter the color the stronger the path weights. The approach A2 produces often false alarms.

significant propagation paths reasonably well. The approach A2 (CUSUM) fails to catch some of the weaker paths (seen from the number of paths remaining below true value in Fig.6), whereas A1 ( $P_{new}$ ) suffers from some false detections (number of paths larger than the true value in Fig.6). The failure to detect weaker paths with the CUSUM-approach is due to the selection of the drift parameter ( $d = 2$  in this example). Choosing lower  $d$  value can cause more false detections, whereas  $d = 2$  in this case obviously prevents weaker paths from reaching the detection threshold. It should also be noted that it can be a question of taste whether a weak path should be interpreted as a concentrated path or as part of the DMC.

From practical point of view the more interesting conclusion lies in the computational load of the two approaches. The right hand side (red curves) in Fig. 6 shows the time taken to process each snapshot. It can be observed that A2 takes in average only 25% of the processing time required by A1.

## V. CONCLUSION

In this paper we discuss the estimation of propagation path parameters using state-space modeling. The emphasis is on the model order selection, i.e., propagation path (target) detection from complex and large nonlinear channel measurements. We propose a path detection algorithm based on the CUSUM method on the whitened residual in delay domain. This approach leads to computational efficient solution which allows

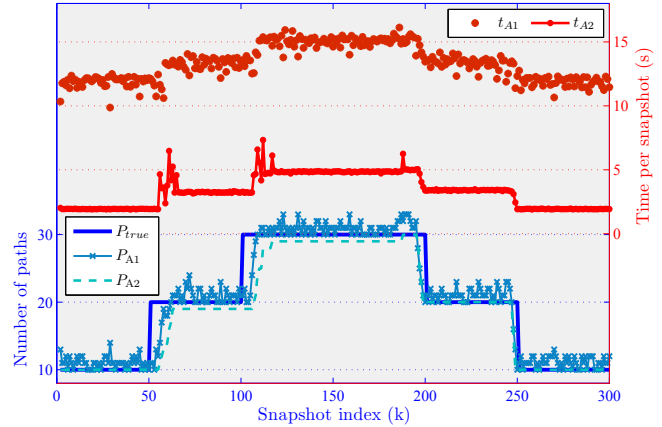


Fig. 6. Left hand axis shows the number of true and estimated propagation paths. A1 estimates also some noise whereas A2 fails to detect weakest paths. Curves related to right hand axis show the time taken to process each observation. A1 is in average 4 times slower than A2.

for a flexible compromise between false alarms and missed detections. Further research is required to derive optimal ways to choose the drift and threshold parameters for different scenarios.

## REFERENCES

- [1] D. Tse and P. Viswanath, *Fundamentals of Wireless Communications*. Cambridge University Press, 2005.
- [2] B. H. Fleury, M. Tschudin, R. Heddergott, D. Dahlhaus, and K. I. Pedersen, "Channel parameter estimation in mobile radio environments using the SAGE algorithm," *IEEE J. Select. Areas Commun.*, vol. 17, no. 3, pp. 434–450, Mar. 1999.
- [3] A. Richter, "Estimation of radio channel parameters: Models and algorithms," Ph. D. dissertation, Technischen Universität Ilmenau, Germany, May 2005, [Online]: [www.db-thueringen.de](http://www.db-thueringen.de).
- [4] A. Richter, M. Enescu, and V. Koivunen, "State-space approach to propagation path parameter estimation and tracking," in *Proc. 6th IEEE Workshop on Signal Processing Advances in Wireless Communications*, New York City, June 2005.
- [5] J. Salmi, A. Richter, M. Enescu, P. Vainikainen, and V. Koivunen, "Propagation parameter tracking using variable state dimension kalman filter," in *Proc. IEEE VTC 2006 Spring*, Melbourne, Australia, May 7-10 2006.
- [6] J. Salmi, A. Richter, and V. Koivunen, "Enhanced tracking of radio propagation path parameters using state-space modeling," in *Proc. EUSIPCO 06*, Florence, Italy, September 2006.
- [7] T. Kaiser, A. Bourdoux, H. Boche, J. R. Fonollosa, J. B. Andersen, and W. Utschick, Eds., *Smart Antennas—State of the Art*. New York, NY: Hindawi Publishing Corporation, 2005.
- [8] M. Steinbauer, A. Molisch, and E. Bonek, "The double-directional radio channel," *IEEE Antennas and Propagation Magazine*, vol. 43, no. 4, pp. 51–63, Aug. 2001.
- [9] A. Richter, J. Salmi, and V. Koivunen, "An algorithm for estimation and tracking of distributed diffuse scattering in mobile radio channels," in *Proc. IEEE International Workshop on Signal Processing Advances in Wireless Communications*, Cannes, France, July 2-5 2006.
- [10] C. B. Ribeiro, A. Richter, and V. Koivunen, "Stochastic maximum likelihood estimation of angle- and delay-domain propagation parameters," in *Proc. of 16th Annual IEEE International Symposium on Personal Indoor and Mobile Radio Communications*, Berlin, Germany, Sep. 2005.
- [11] F. Gustafsson, *Adaptive Filtering and Change Detection*. Chichester, England: John Wiley and Sons, Ltd., 2000.
- [12] R. G. Brown and P. Y. Hwang, *Introduction to Random Signals and Applied Kalman Filtering*, 3rd ed. New York, NY: John Wiley and Sons Inc., 1997.
- [13] S. M. Kay, *Fundamentals of Statistical Signal Processing: Detection Theory*. Prentice-Hall International, 1998, vol. 2.